Monitoring and Inhibition of Plk1: Amphiphilic porphyrin conjugated Plk1 specific peptides for its imaging and anti-tumor function

Hongguang Li,[a] Chi-Fai Chan,[a] Wai-Lun Chan,[a] Sam Lear,[b] Kwok-Keung Shiu,[a] Steven L. Cobb,[b] Nai-Ki Mak,[c] Terrence Chi-Kong Lau,[d] Rongfeng Lan,[e*] Wai-Kwok Wong,[a*] and Ka-Leung Wong [a*]

[a] Department of Chemistry, Hong Kong Baptist University, Kowloon Tong, Hong Kong SAR; [b] Department of Chemistry, Durham University, Durham, DH1 3LE, UK; [c] Department of Biology, Hong Kong Baptist University, Kowloon Tong, Hong Kong SAR; [d] Department of Biology and Chemistry, City University of Hong Kong, Kowloon Tong, Hong Kong SAR; [e] Hong Kong Baptist University Institute of Research and Continuing Education, Shenzhen, P. R. China.

Supporting Information

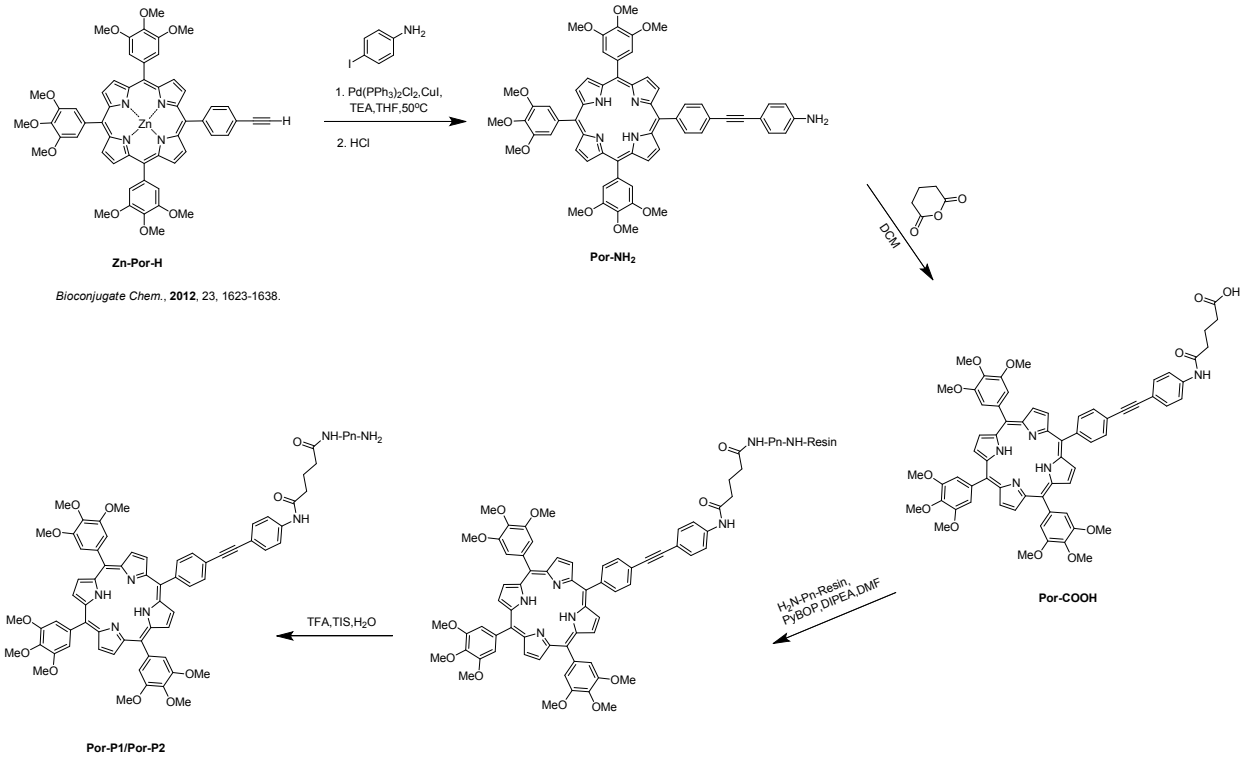

Figure S1.The synthetic scheme for Por-**P1** and Por-**P2**.

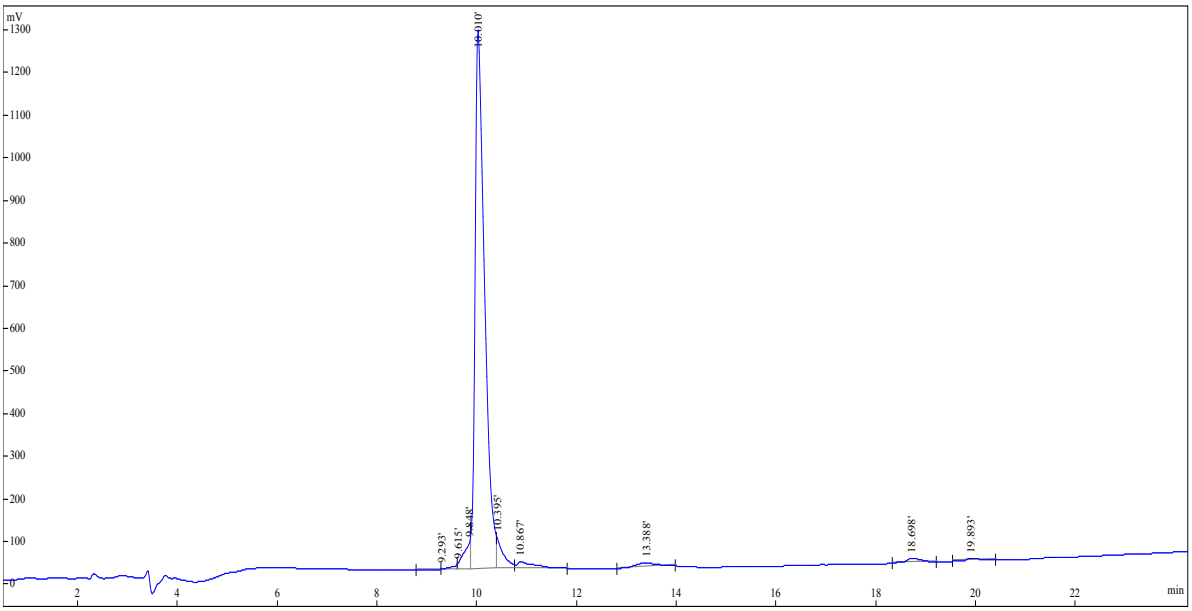

Figure S2. HPLC trace of **P1**- condition 10% A (ACN+0.1%TFA) + 90% B (H_2O+0.1%TFA).

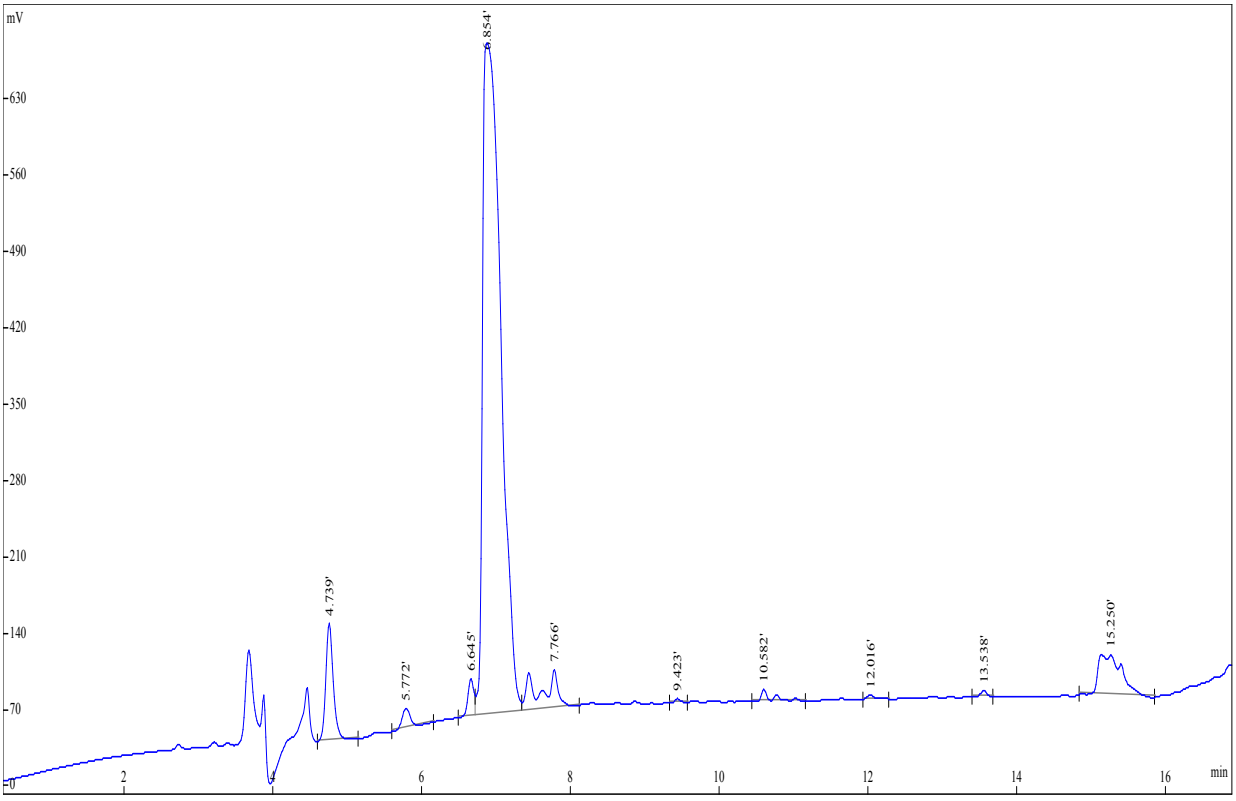

Figure S3. HPLC trace of **P2**- condition 10% A (ACN+0.1%TFA) + 90% B (H_2O+0.1%TFA).

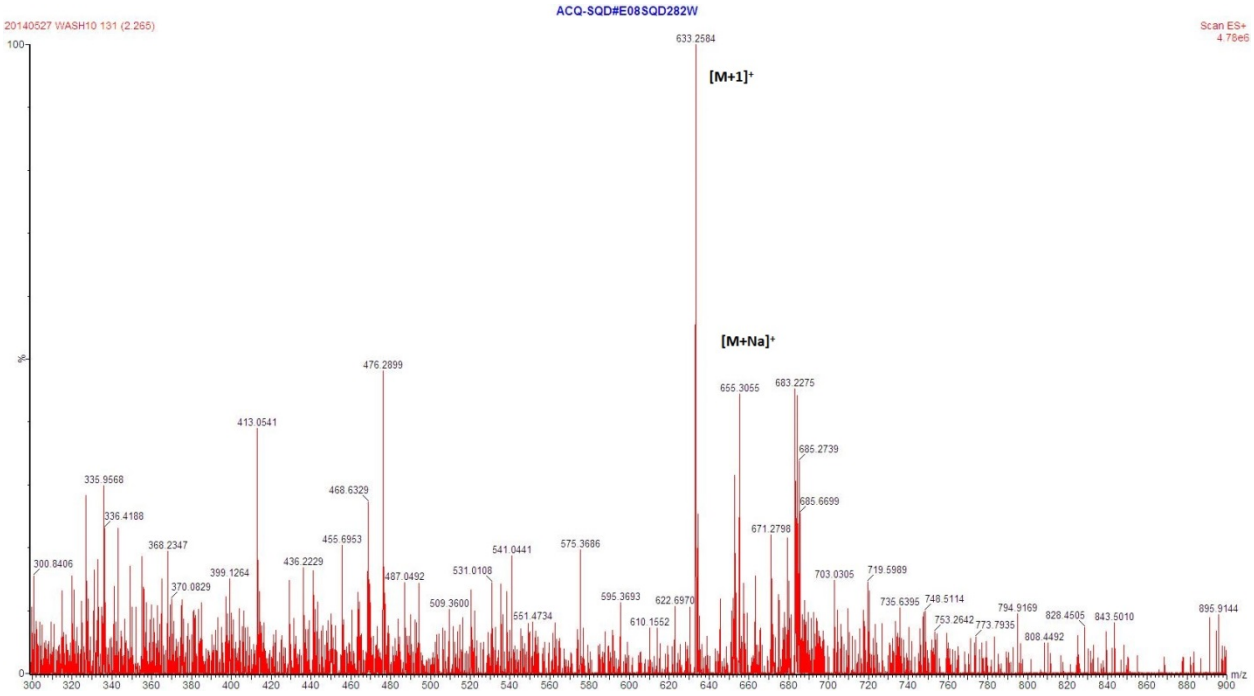

Figure S4. ESI-MS spectrum of **P1**.

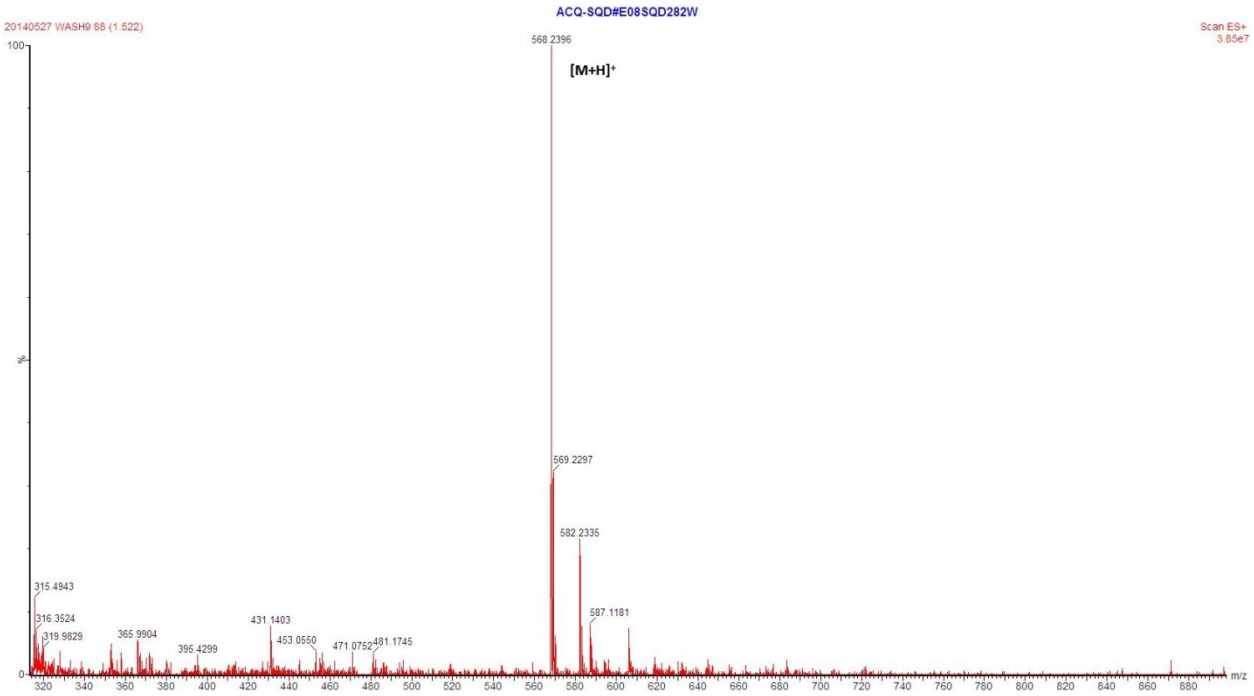

Figure S5. ESI-MS spectrum of **P2**.

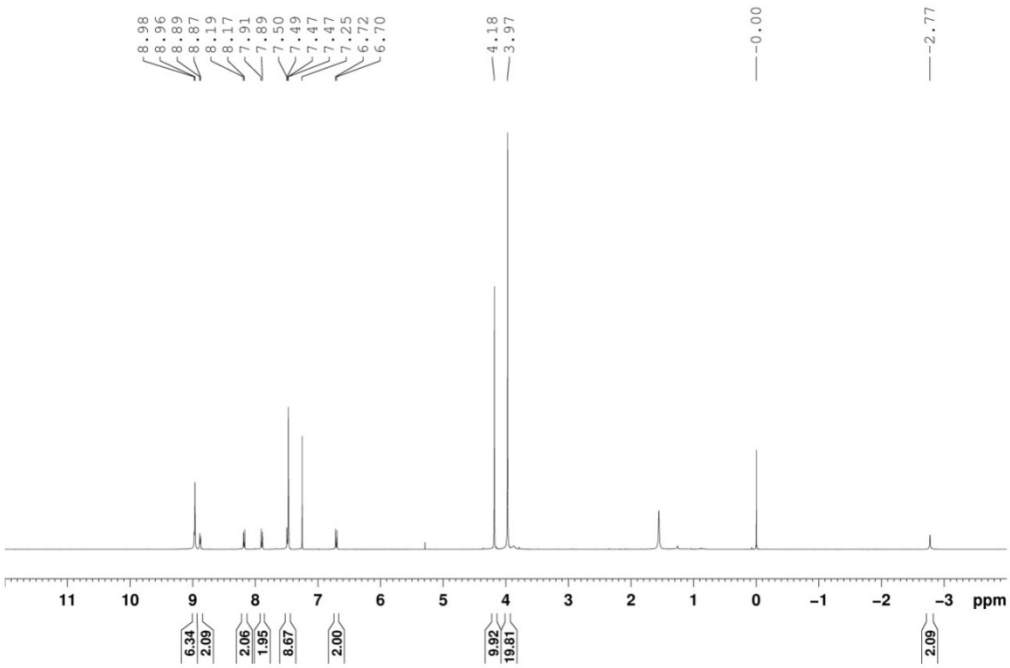

FigureS6. ^{1}H-NMR spectrum of Por-NH_2.

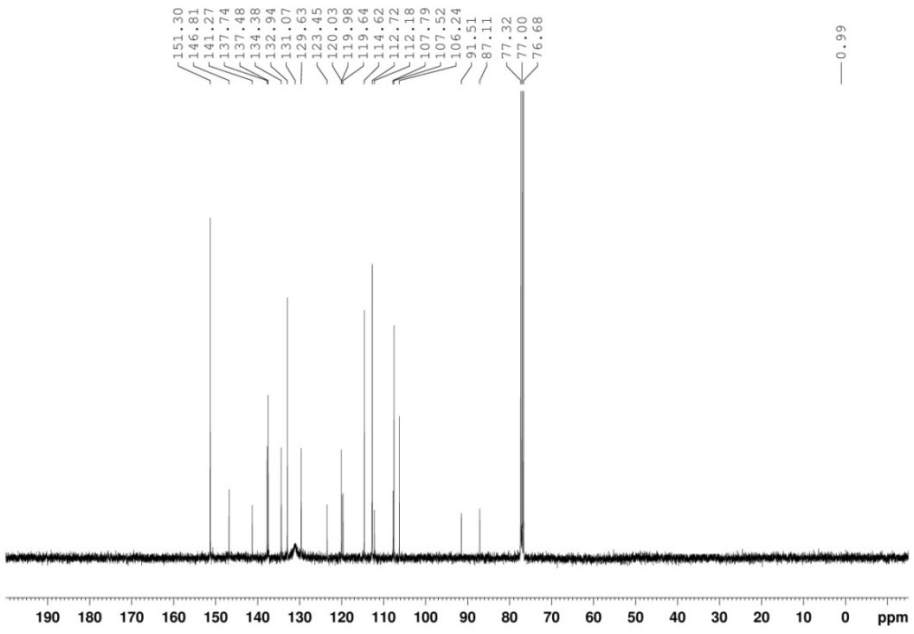

FigureS7. ^{13}C-NMR spectrum of Por-NH_2.

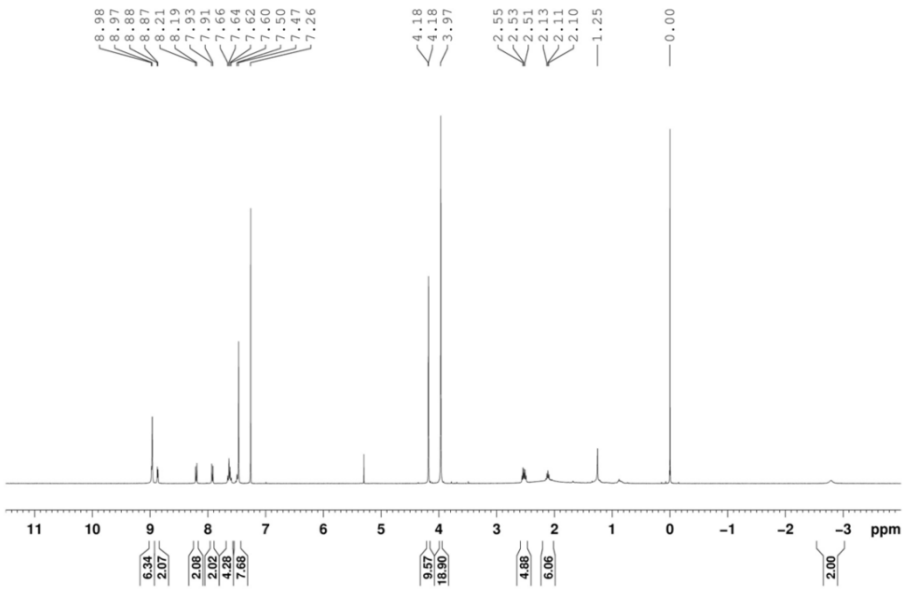

FigureS8. ^{1}H-NMR spectrum of Por-COOH.

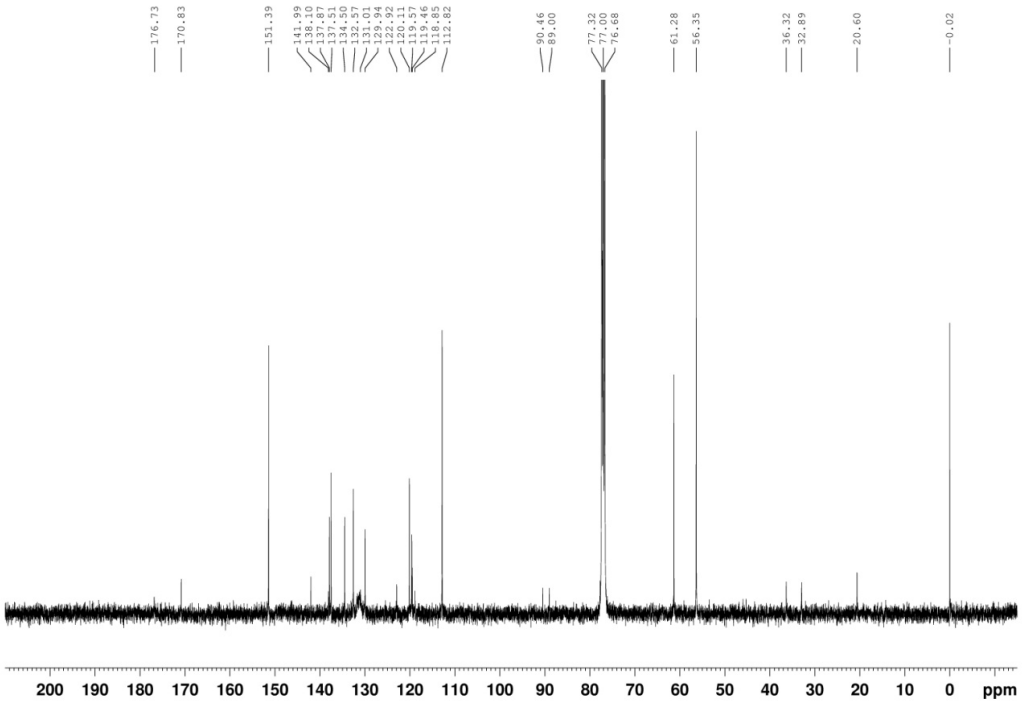

FigureS9. ^{13}C-NMR spectrum of Por-COOH.

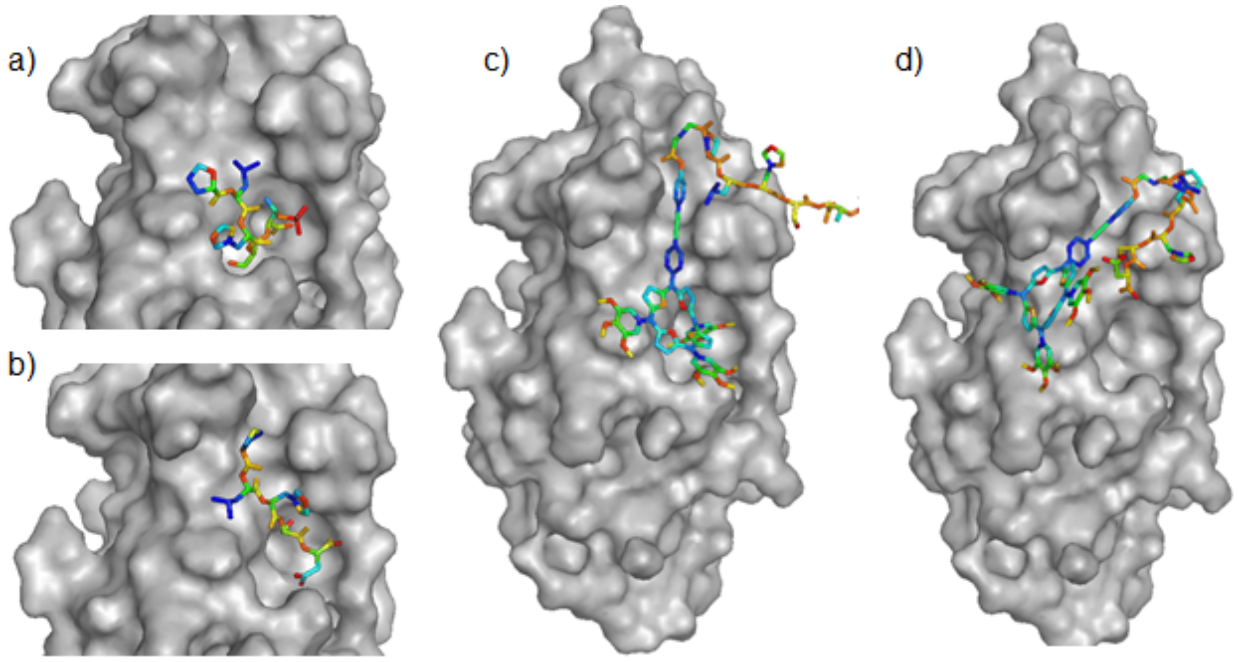

Figure S10. The binding fitting via molecular modeling for the comparisons of interactions between (a) **P1**, (b) **P2**, (c) Por-**P1**, (d) Por-**P2** and Plk1 structure.

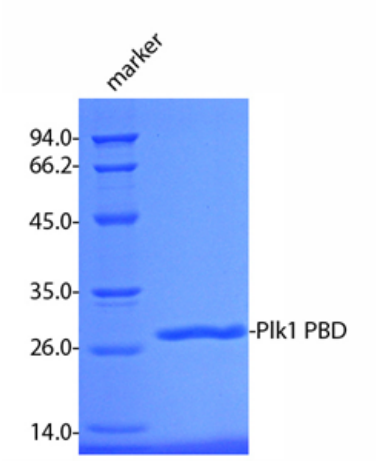

FigureS11. Purified Plk1 (PBD domain) in protein gel stained with coomassie blue.

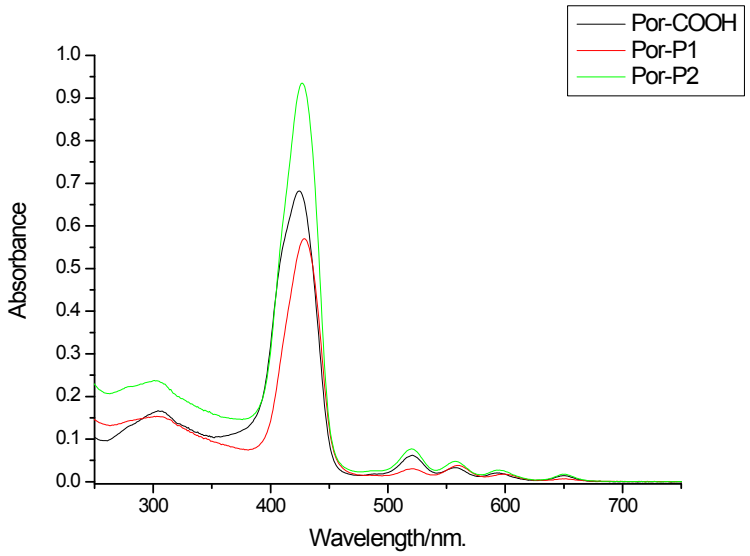

Figure S12.The UV absorption spectra of Por-COOH, Por-**P1** and Por-**P2** (10^{-5}M) in HEPES buffer (10 mM HEPES, pH=8.0, 150 mM NaCl).

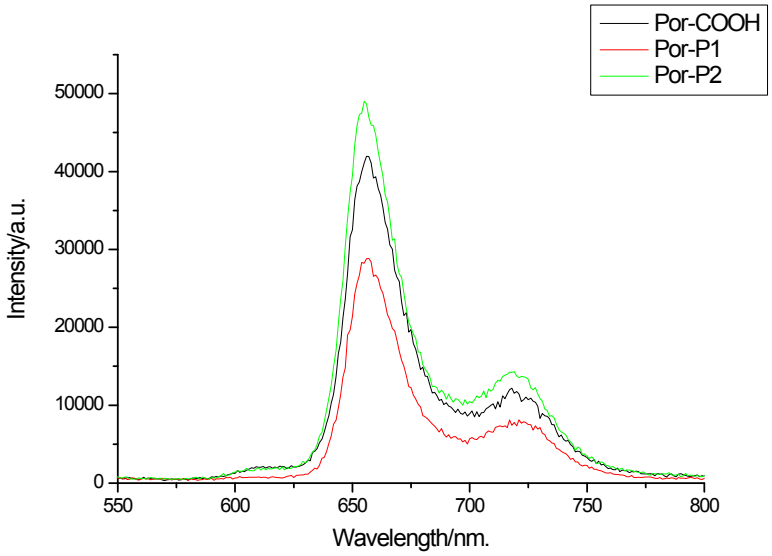

Figure S13. The emission spectra of Por-COOH, Por-**P1** and Por-**P2** in HEPES buffer. (λ_{ex} = 430 nm and 10^{-6}M)

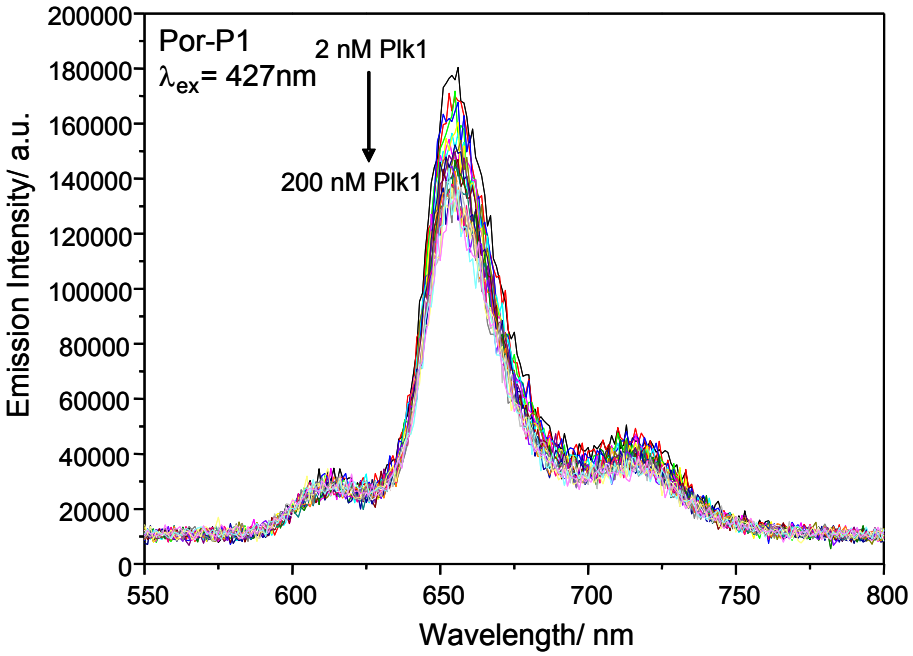

FigureS14. The emission titration of Por-**P1** (1 μM) upon addition of Plk1 (2 nM - 200 nM) in HEPES buffer. (λ_{ex} = 427 nm)

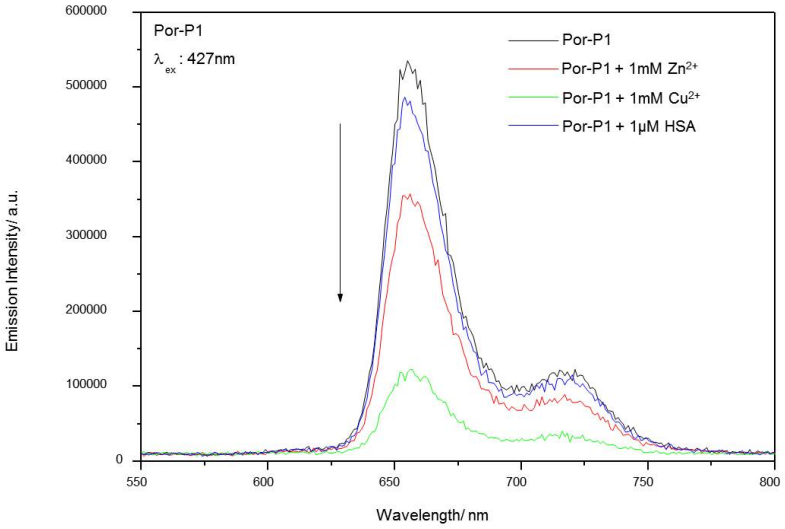

Figure S15. The emission change of Por-**P1** (1 μM) upon addition of Zn^{2+}, Cu^{2+} and HSA in HEPES. (λ_{ex} = 427 nm)

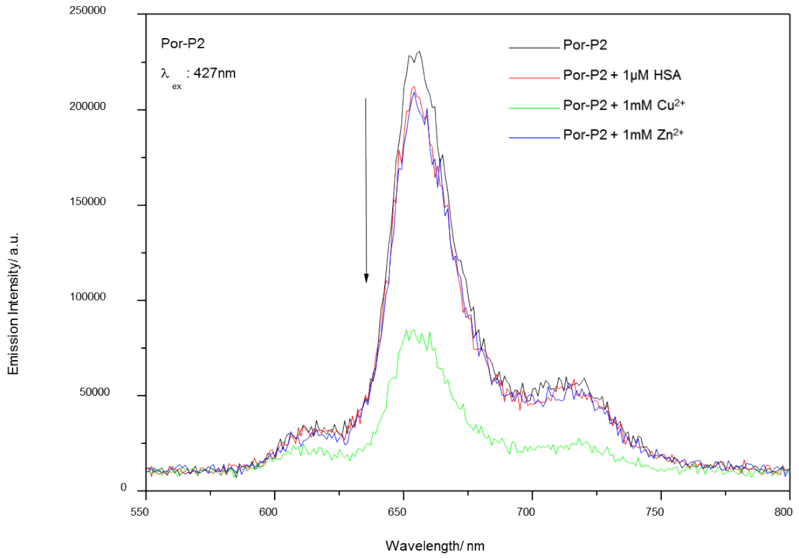

Figure S16. The emission change of Por-**P2** (1 μM) upon addition of Zn^{2+}, Cu^{2+} and HSA in HEPES buffer. (λ_{ex} = 427 nm)

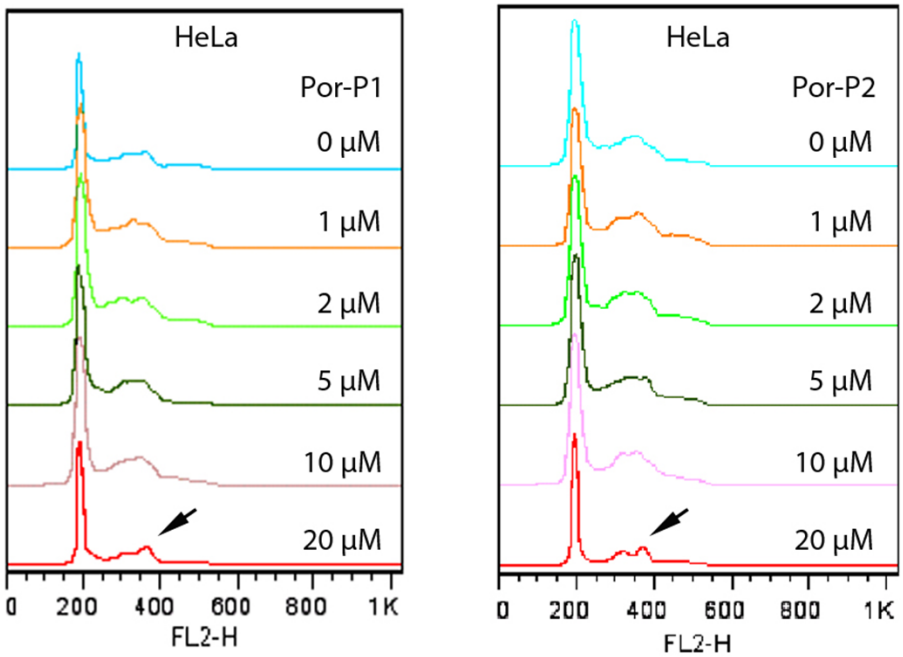

Figure S17. Representative Half-Offset histograms of HeLa cells analyzed by Flow cytometry after treated with Por-**Pn**. Figures were processed by using FlowJo 7.6.1. Por-**P1** or Por-**P2** cause the HeLa cells arrested in G2/M phase in a concentration-dependent manner, with an obvious G2/M peak in the concentration of 20 μM.

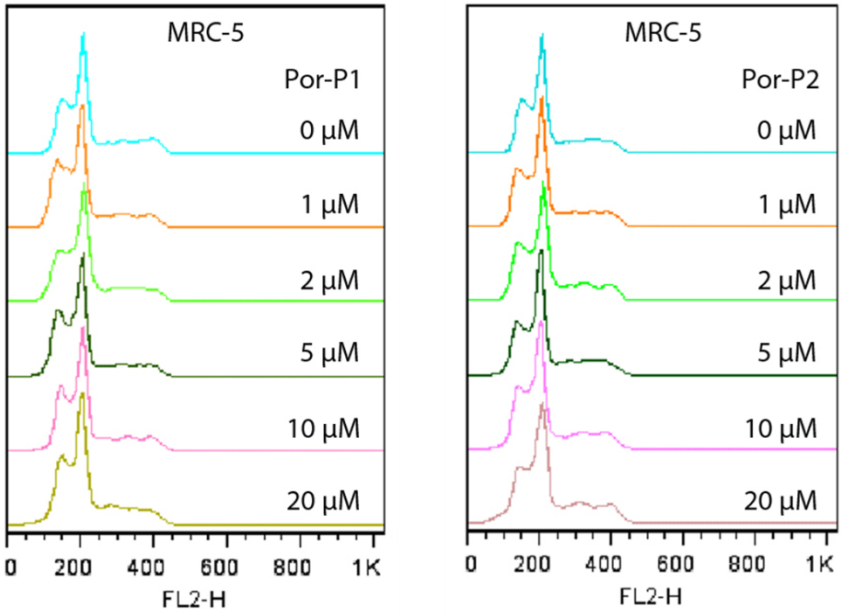

Figure S18. Raw data of MRC-5 cells analyzed using Flow cytometry and presented by Half-Offset histograms from FlowJo 7.6.1. Parallel performed as in **Figure S17**.

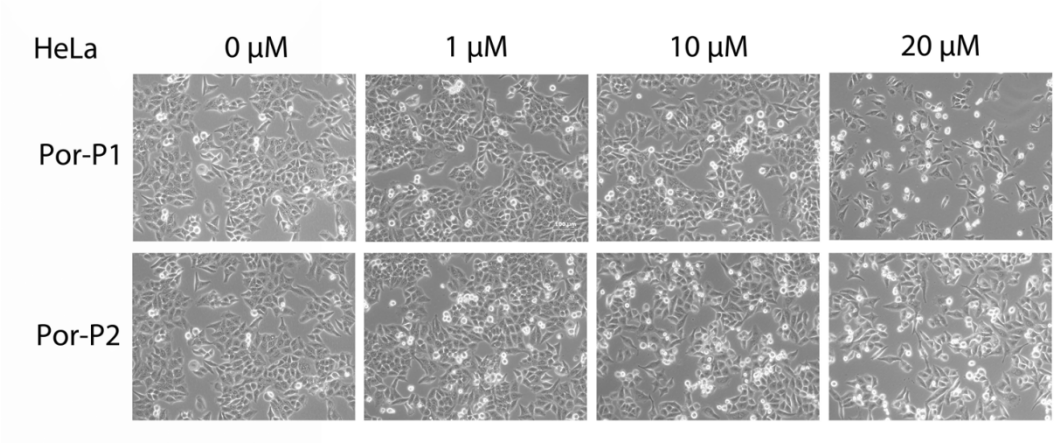

Figure S19. Por-**P1** and Por-**P2** treatments had induced Plk1 inhibition and succeeding G2/M arrest of HeLa cells. Experimentally, HeLa cells were microscopically imaged by Zeiss Axio Observer A1 (10 ×).Upon 10 or 20 μM of Por-Pn treatments, parts of cells showed mitotic arrested, and cell growth was inhibited.

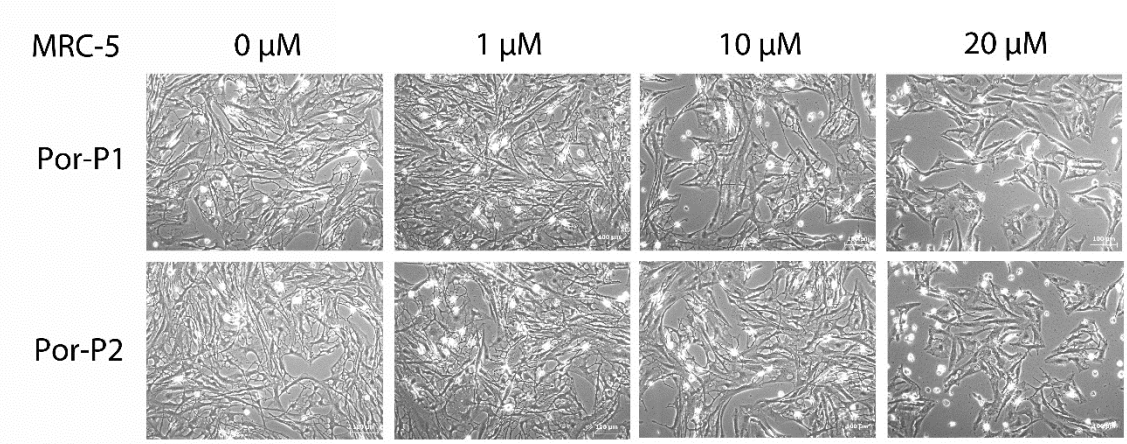

Figure S20. Human normal lung fibroblasts MRC-5 cells were treated with Por-**P1** and Por-**P2** and then microscopically imaged. No obvious effects were detected under Por-**Pn** treatments on the MRC-5 cells.